

## Anisotropic heat transport in the octylcyanobiphenyl (8CB) liquid crystal

M. Marinelli,\* F. Mercuri, S. Foglietta, U. Zammit, and F. Scudieri

*Dipartimento di Ingegneria Meccanica, 2° Università di Roma and Sezione INFM, Tor Vergata,  
Via della Ricerca Scientifica e Tecnologica, 00133 Roma, Italy*

(Received 29 February 1996)

The critical behavior of the specific heat, thermal conductivity, and thermal diffusivity at the smectic-A–nematic phase transition of aligned octylcyanobiphenyl (8CB) has been studied with the photopyroelectric technique. Though the values of the thermal transport parameters are substantially different for homeotropic and planar alignment, it has been shown that the thermal diffusivity critical behavior is characterized by the same critical exponent in the two cases. This result suggests that the mode couplings that govern the critical dynamics associated with the thermal parameters are isotropic. The thermal conductivity remains substantially flat, with only a minor increase close to the transition temperature. [S1063-651X(96)06307-6]

PACS number(s): 64.70.Md

### INTRODUCTION

One of the unresolved questions regarding the smectic-A–nematic (AN) phase transition in liquid crystals is the one related to the anisotropic critical behavior observed in the correlation length ( $\xi$ ) compared with the isotropic one found in the specific heat ( $c$ ) [1]. In particular, it has been shown [2] that in compounds where the McMillan ratio  $T_{AN}/T_{NI}$  ( $T_{AN}$  and  $T_{NI}$  being the AN and nematic-isotropic transition temperatures) is less than 0.93, the critical behavior of  $c$  can be described by the isotropic three-dimensional (3D)  $XY$  model which predicts  $\alpha_{XY} = -0.007$  and  $A'/A = 0.9714 \pm 0.0126$  [3]. On the other hand, the correlation length perpendicular and parallel to the normal to the smectic layers shows anisotropic critical behavior at the AN transition [4], with the critical exponents  $\nu_{\parallel} \neq \nu_{\perp} \neq \nu_{XY}$ . Attempts have been made in the past to solve this problem, and a gauge transformation theory [5] was eventually able to account for the critical anisotropy in  $\xi$ . This theory, however, predicted an inverted 3D  $XY$ -like behavior for the specific heat for compounds with a large nematic range never observed experimentally [2]. More recently, a self-consistent one loop theory [6] which is based on an intrinsically anisotropic coupling between the fluctuations of the nematic order parameter  $\delta n$  and the smectic order parameter  $\psi$ , has been developed. This theory predicts a crossover from isotropic to anisotropic critical behavior for materials with increasing McMillan ratio. In particular, for materials with  $T_{AN}/T_{NI} < 0.93$ , for which the specific-heat data are consistent with the isotropic 3D  $XY$  model, the one loop theory predicts a weak anisotropy. Finally, according to the theory an isotropic critical behavior for  $\xi$  should be observed, but in compounds with a  $T_{AN}/T_{NI}$  value much smaller than the ones available up to now.

It is well known that thermal transport parameters such as the thermal diffusivity  $D$  and the thermal conductivity  $k$  are anisotropic in the smectic and nematic phases of liquid crystals [7]. For example, in *MBBA* it turns out that  $D_{\parallel}$  is about two times larger than  $D_{\perp}$  for  $T < T_{NI}$ . The question is

whether the critical behaviors of  $D$  and  $k$  over the AN transition are also anisotropic; in other words, whether these quantities behave as the correlation length or as the specific heat. The question may arise since, according to a simple model developed in Ref. [8] for the thermal diffusivity of an extended mean-field-like smectic-A–smectic-C (AC) transition, a dependence of  $D$  on  $\xi$ , whose critical behavior is isotropic for such a transition, is obtained. Measurements for  $D$  and  $k$  close to  $T_{AN}$  are available in the literature [9], but they have been obtained in nonaligned samples. It has been found that  $k$  remains flat while  $D$  has a critical exponent which is approximately equal to that of the specific heat. It must be noted that the anisotropy in the values of  $D$  and  $k$ , which is essentially due to the shape anisotropy of the liquid crystal molecules, has nothing to do with eventual anisotropies in their critical behavior, which is associated with the coupling between long lived modes [10]. In the case of nonaligned samples the data have been explained on the basis of a model that considers isotropic dissipative coupling between the order parameter and the heat diffusion mode [9].

In the present paper we shall report on the simultaneous measurement of  $c$ ,  $k$ , and  $D$  of octylcyanobiphenyl (8CB) samples with planar and homeotropic alignments. The critical behavior of  $c$  at the AN transition confirms, for this compound, the data already reported in the literature [11] that shows a crossover from 3D  $XY$  to tricritical critical behavior. The temperature dependences of the values of  $D_{\parallel}$  and  $D_{\perp}$  have been measured in the temperature range from 29 to 45 °C, and the results which have been found are very similar to the one obtained for other compounds [7]. High resolution measurements close to the AN transition show that the critical exponent of  $D$  is approximately the same for samples with planar and homeotropic alignments, and it is therefore concluded that the critical behavior of the transport thermal parameters is isotropic. In both cases the thermal conductivity remains smooth, with only a minor increase close to  $T_{AN}$  whose origin is at present not clear.

### EXPERIMENT

A standard photopyroelectric setup [12] has been used to perform the measurements. The sample was sandwiched be-

\*Electronic address: marinelli@utovrm.it

tween a 300- $\mu\text{m}$ -thick Z-cut  $\text{LiTaO}_3$  pyroelectric transducer and a glass plate whose surface in contact with the liquid crystal was coated with a 300-nm-thick metallic overlayer (optically opaque and thermally thin). The thickness of the sample was 30  $\mu\text{m}$ . Light from an acoustooptically modulated He-Ne laser was absorbed by the very thin metallic coating in contact with one of the liquid crystal surfaces, and the temperature oscillations introduced in the sample were detected on the opposite sample surface by the transducer. The modulation frequencies were 62 and 36 Hz for homeotropic and planar alignments, respectively. The amplitude and phase of the pyroelectric signal were analyzed by a two phase lock-in amplifier. When the sample is optically opaque and thermally thick [13], it has been shown that two of the three quantities  $c$ ,  $k$ , and  $D$  can be simultaneously obtained from the amplitude and phase of the signal, and the third calculated from their relation  $D=k/\rho c$  [12]. A thermally thick sample means that the thermal diffusion length ( $\mu = \sqrt{D/\pi f}$ ) is much smaller than the sample thickness  $l$ . This condition can therefore be fulfilled using a suitable modulation frequency  $f$ . The validity of the conditions under which the thermal parameters can be simultaneously determined can be checked experimentally performing a frequency scan [12]. It has moreover been shown that from such a scan the determination of the absolute value of  $D$  can be easily obtained [12]. A negative lens was used to spread the laser light on the sample surface to control the power density impinging on the sample. The power density and the temperature rate change were decreased as much as possible to minimize the influence of thermal gradients on the measurements. The laser spot on the sample surface was much larger than the sample thickness to ensure one dimensional geometry for the heat flow. The adopted measuring procedure requires a calibration at a temperature where the values of sample thermal parameters are known. We used specific-heat values from Ref. [11], and measured the absolute values of  $D$  at the same temperatures with frequency scans. A planar alignment of the sample was obtained by means of  $\approx 100\text{-nm}$   $\text{SiO}_2$  film sputtered on the cell walls at an angle of  $\approx 60^\circ$  with respect to the normal to the sample surface. The homeotropic alignment was obtained treating the sample cell walls with a solution of trimethylcetylammmonium bromide.

## RESULTS

Figure 1 shows the specific heat data over the temperature range 29–45  $^\circ\text{C}$  for samples aligned in the two directions. The second order AN phase transition and the weakly first order NI transition are clearly visible, and the data agree with the ones available in literature [11]. As expected, there are no significant differences between the two data sets which superimpose quite well over the whole temperature range.

Figure 2 shows  $D_{\parallel}$  and  $D_{\perp}$  vs temperature. Both quantities show a dip at  $T_{\text{NA}}$  and  $T_{\text{NI}}$ , but they have significantly different values in the nematic and smectic phases. The data, on the other hand, superimpose in the disordered phase. The two thermal diffusivity data sets have been obtained from the phase data measured as a function of temperature, and the corresponding calibration absolute values obtained at  $\sim 45^\circ\text{C}$  by frequency scans. The squares in Fig. 2 represent additional absolute values of  $D$  obtained performing fre-

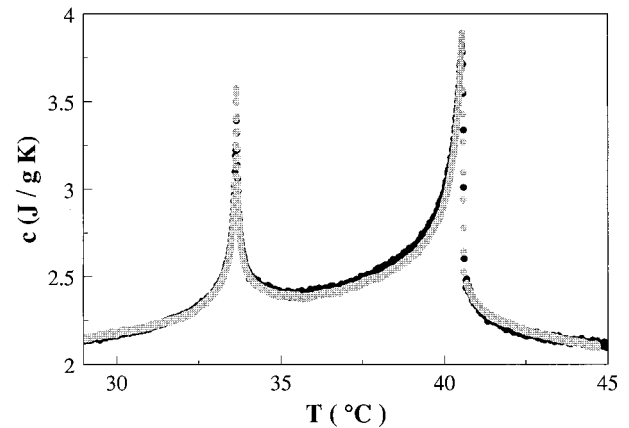


FIG. 1. 8CB specific heat behavior vs temperature for planar (light grey dots) and homeotropic (dark dots) aligned samples.

quency scans at fixed sample temperatures to crosscheck against any anomalous systematic vs temperature behavior of the experimental setup. There is an excellent agreement among the data obtained in this way and the ones vs temperature scans, showing the reliability of the measurements. The  $D_{\parallel}$  and  $D_{\perp}$  vs temperature data we have obtained are similar to the thermal diffusivity data reported in Ref. [7]. It should be noted, however, that the resolution of the measurements in that case was not so high, since it was not possible to detect the NA transition, which can be easily detected by the pyroelectric technique.

Figure 3 shows  $k_{\parallel}$  and  $k_{\perp}$  temperature scans. Again the data relative to both orientations superimpose quite well in the isotropic phase, while  $k_{\parallel}$  is significantly larger than  $k_{\perp}$  in the nematic and smectic phases. An increase in  $k_{\parallel}$  and a decrease in  $k_{\perp}$  are clearly evident on cooling below the NI transition, while no significant changes can be detected near the NA transition. The results reported in Figs. 1–3 were obtained with a temperature rate change of 20 mK/min, and the data were taken every 5 mK. Hereafter high-resolution measurements with a temperature rate change of 0.5 mK/min and data taken every 0.3 mK over a narrower temperature region close to the NA transition will be presented and dis-

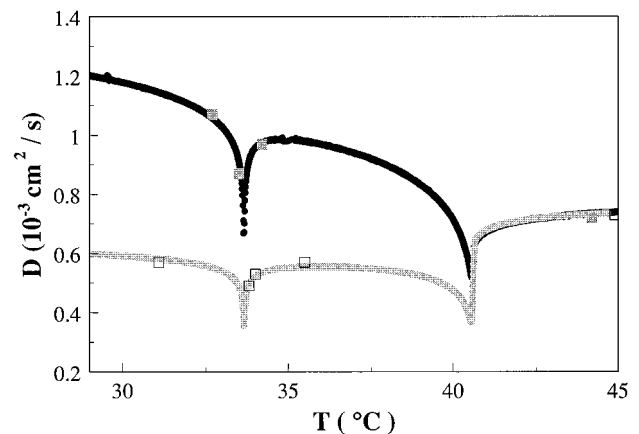


FIG. 2. 8CB thermal diffusivity behavior vs temperature for planar (light grey dots) and homeotropic (dark dots) aligned samples. Squares represent thermal diffusivity absolute values obtained from frequency scans at fixed temperatures.

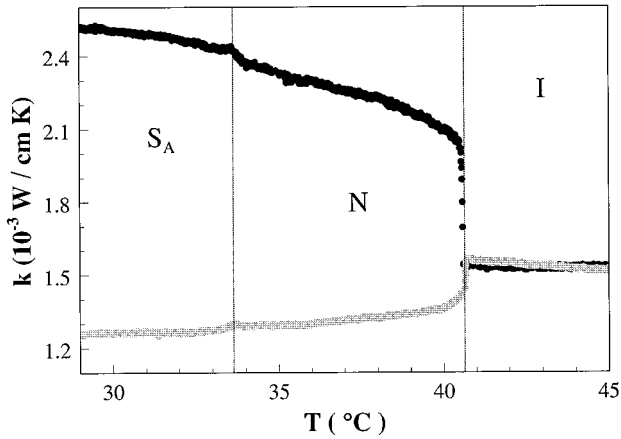


FIG. 3. 8CB thermal-conductivity behavior vs temperature for planar (light grey dots) and homeotropic (dark dots) aligned samples.

cussed for the study of the static as well as dynamic critical behavior associated with the thermal parameters over the phase transition.

Figures 4(a) and 4(b) show the specific heat data vs reduced temperature for the homeotropic and planar alignments, respectively. The data have been fitted using the expression

$$c = B + E(T - T_c) + A^\pm |T - T_c|^{-\alpha} (1 + D^\pm |T - T_c|^{0.5}), \quad (1)$$

where + refers to  $T > T_c$  and - to  $T < T_c$ . The solid lines in Figs. 4(a) and 4(b) correspond to Fit 1A and Fit 1B in Table

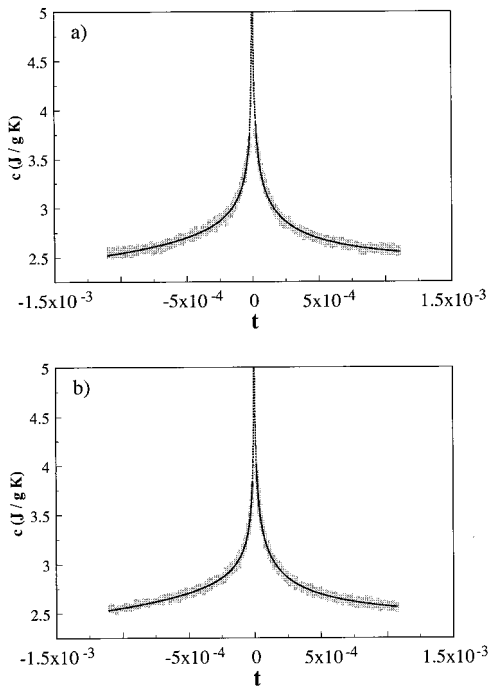


FIG. 4. 8CB specific heat behavior vs reduced temperature  $t = (T - T_c)/T_c$  for homeotropic (a) and planar (b) aligned samples. Light grey squares represent the experimental data. Solid lines correspond to the fits 1A and 1B of Table I. The dotted lines correspond to the reduced temperature regions which have not been considered in the fits.

I, respectively. The two fits are, as expected, almost identical: the differences in the critical exponent and amplitude ratio, in particular, are well within the statistical uncertainties. These values ( $\alpha = 0.31 \pm 0.03$  and  $A^+/A^- = 1.20 \pm 0.05$ ) are moreover in very good agreement with the ones reported in Ref. [11]. As already stated, the specific heat data at the AN transition can be well described by the 3D XY model if  $T_{AN}/T_{NI} < 0.93$ . In the case of 8CB,  $T_{AN}/T_{NI} = 0.98$ , and therefore a crossover from 3D XY to tricritical behavior is expected, leading to  $\alpha > \alpha_{XY}$ .

Figures 5(a) and 5(b) show  $k_{\parallel}$  and  $k_{\perp}$  vs reduced temperature. Both are rather smooth over all the investigated reduced temperature range, though their absolute values are different. Figures 6(a) and 6(b) show  $D_{\parallel}$  and  $D_{\perp}$  vs reduced temperature. The data have been fitted using the fitting expression

$$D = \frac{H + G(T - T_c)}{B + E(T - T_c) + A^\pm |T - T_c|^{-\alpha} (1 + D^\pm |T - T_c|^{0.5})}. \quad (2)$$

This choice of the fitting function originates from the assumption of an approximately linear behavior of  $k$ . We have first tried to fix  $B$ ,  $E$ ,  $A^\pm$ ,  $T_c$ ,  $\alpha$ , and  $D^\pm$  at the values obtained from fit 1A for  $D_{\parallel}$  and from 1B for  $D_{\perp}$ ,  $H$ , and  $G$  being the only adjustable parameters. The obtained results correspond to fits 2A and 2B in Table I, respectively, but their quality is rather poor as shown by the  $\chi^2_v$  values. We have then released all the parameters, and fits 3A and 3B in Table I show the results. With small adjustments of the parameters, we obtained a very good  $\chi^2_v$ , and therefore a good fit. The difference in  $\alpha$  between fits 1A, 3A and 1B, 3B are within the statistical uncertainties, as are all variations in the other parameters. We have also tried to fix  $\alpha = 0.31$  for the planar sample and  $\alpha = 0.32$  for the homeotropic one, and also obtained good fits (fits 4A and 4B). As already stated, the choice of Eq. (2) is based on the assumption of a linear  $k$  dependence vs  $t$ . However, from Fig. 5, which shows  $k$  data in an expanded scale, it must be noted that this assumption is somewhat too simplified. In fact, fitting  $k$  data with a linear dependence for both orientations (Fits 5A and 5B in Table I), we obtained the solid lines in Figs. 5(a) and 5(b). These fits are not of very high quality, as can be deduced from the  $\chi^2_v$  values.

## DISCUSSION

The specific-heat data confirm the results already reported in literature on 8CB at the AN transition [11]. The critical behavior is dominated by a crossover from the 3D XY to tricritical, and this is the reason why the obtained  $\alpha$  values are significantly larger than  $\alpha_{XY}$ . The results obtained for the absolute values of  $D$  confirm the well known anisotropy in the thermal transport properties [7]. A value of  $D_{\parallel}$  which is approximately two times larger than the  $D_{\perp}$  one has been obtained for  $T < T_{NI}$ . It has been shown that, because of the rodlike shape of liquid crystal molecules, the thermal diffusivity along a direction parallel to the long axis of the molecule is larger than the one in every other direction. Our results are in qualitative agreement with the ones already reported by Rondelez and co-workers [7], which showed a  $D_{\parallel}$  value about a factor 2 larger than  $D_{\perp}$  in *MBBA* and *OBBA* at temperatures below the clearing point [7]. Moreover, our results confirm that the  $D$  critical behavior at the AN transition is essentially associated with the one of the

TABLE I. Fitting parameters for the specific heat (fit 1), thermal diffusivity (fits 2–4), and thermal conductivity (fit 5) for homeotropic (A) and planar (B) alignments, respectively.

Fit	$\alpha$	$A^+/A^-$	$T_c$ (K)	$B$ (J/g K)	$E$ (J/g K)	$A^-$ (J/g K)	$D^-$	$D^+$	$H$ (W/cm K)	$G$ (W/cm K <sup>2</sup> )	$\chi_p^2$
1A	0.32 $\pm 0.04$	1.1 $\pm 0.1$	306.797 $\pm 0.005$	2.24 $\pm 0.08$	0.2 $\pm 0.4$	0.31 $\pm 0.09$	-0.2 $\pm 0.8$	-0.9 $\pm 0.8$			1.09
2A	(fixed at the same values as Fit 1A)								$(2.412 \pm 0.006) \times 10^{-3}$	$(-1.287 \pm 0.007) \times 10^{-4}$	6.02
3A	0.34 $\pm 0.02$	1.1 $\pm 0.1$	306.798 $\pm 0.002$	2.18 $\pm 0.09$	$(0 \pm 1) \times 10^{-3}$	0.30 $\pm 0.04$	0.3 $\pm 0.4$	0.0 $\pm 0.4$	$(2.51 \pm 0.04) \times 10^{-3}$	$(-1.72 \pm 0.01) \times 10^{-4}$	1.02
4A	0.32 (fixed)	1.08 $\pm 0.09$	306.798 $\pm 0.002$	1.96 $\pm 0.08$	0.10 $\pm 0.01$	0.38 $\pm 0.04$	0.6 $\pm 0.2$	0.3 $\pm 0.3$	$(2.52 \pm 0.01) \times 10^{-3}$	$(-6.8 \pm 0.1) \times 10^{-5}$	1.03
5A									$(2.424 \pm 0.001) \times 10^{-3}$	$(-7.6 \pm 0.6) \times 10^{-5}$	1.28
1B	0.31 $\pm 0.03$	1.2 $\pm 0.2$	306.795 $\pm 0.002$	2.25 $\pm 0.09$	0.2 $\pm 0.4$	0.30 $\pm 0.09$	-0.3 $\pm 0.7$	-0.9 $\pm 0.9$			1.01
2B	(fixed at the same values as the Fit 1B)								$(1.31 \pm 0.01) \times 10^{-3}$	$(6 \pm 5) \times 10^{-5}$	5.30
3B	0.33 $\pm 0.03$	1.2 $\pm 0.1$	306.795 $\pm 0.001$	2.25 $\pm 0.08$	0.26 $\pm 0.09$	0.27 $\pm 0.04$	0.0 $\pm 0.5$	-0.8 $\pm 0.5$	$(1.31 \pm 0.04) \times 10^{-3}$	$(5 \pm 5) \times 10^{-5}$	0.98
4B	0.31 (fixed)	1.18 $\pm 0.09$	306.795 $\pm 0.001$	2.17 $\pm 0.08$	-0.1 $\pm 0.1$	0.35 $\pm 0.06$	0.5 $\pm 0.3$	-0.3 $\pm 0.3$	$(1.38 \pm 0.05) \times 10^{-3}$	$(-1.4 \pm 0.6) \times 10^{-4}$	0.98
5B									$(1.305 \pm 0.004) \times 10^{-3}$	$(3 \pm 1) \times 10^{-5}$	1.25

specific heat, as already reported for the same transition of  $\bar{8}S5$  [9]. The result from our measurements is that the critical behavior of the thermal transport parameters is isotropic.  $D_{\parallel}$  and  $D_{\perp}$  have the same critical behavior over  $T_{AN}$  in spite of their absolute values being significantly different. This means that all couplings among long lived modes, relevant for the critical dynamic associated with the thermal transport properties of the system, are isotropic, and that the anisotropy in the critical behavior of the correlation length does not affect the critical behavior of the thermal transport parameters. As already mentioned, high resolution thermal diffusivity data at the AN transition have been already reported for  $\bar{8}S5$  [9], and approximately equal critical exponents for  $c$  and  $D$  were obtained. This result was explained in terms of a theoretical model for critical dynamics [9] which consider a dissipative coupling between the order parameter and the conserved energy density of the system. Similarly, in the case of 8CB, the critical behavior of the thermal diffusivity is also determined by the specific heat critical exponent as shown in the fit results. It should be noted, however, that  $\bar{8}S5$  has a McMillan ratio  $T_{NA}/T_{NI}=0.94$ , and the coupling between the nematic  $S$  and the smectic order parameter  $\psi$  in  $\bar{8}S5$  is negligible with respect to the one between  $\psi$  and the fluctuations of the nematic order parameter  $\delta n$ . In 8CB, with increasing McMillan ratio, the  $S$  and  $\psi$  coupling becomes important, and a crossover to the tricritical behavior is expected. This is the reason why  $\bar{8}S5$  has  $\alpha=-0.022$ , which is much closer to  $\alpha_{XY}$  with respect to 8CB, where  $\alpha=0.31-0.32$ . The presence of such a crossover in statics with increasing  $T_{NA}/T_{NI}$  does not automatically imply that additional kinds of couplings between the heat diffusion mode and other long lived modes comes into play in the critical dynamics of the AN transition when the tricritical point is approached, possibly affecting the critical behavior of the thermal diffusivity. However, it should be

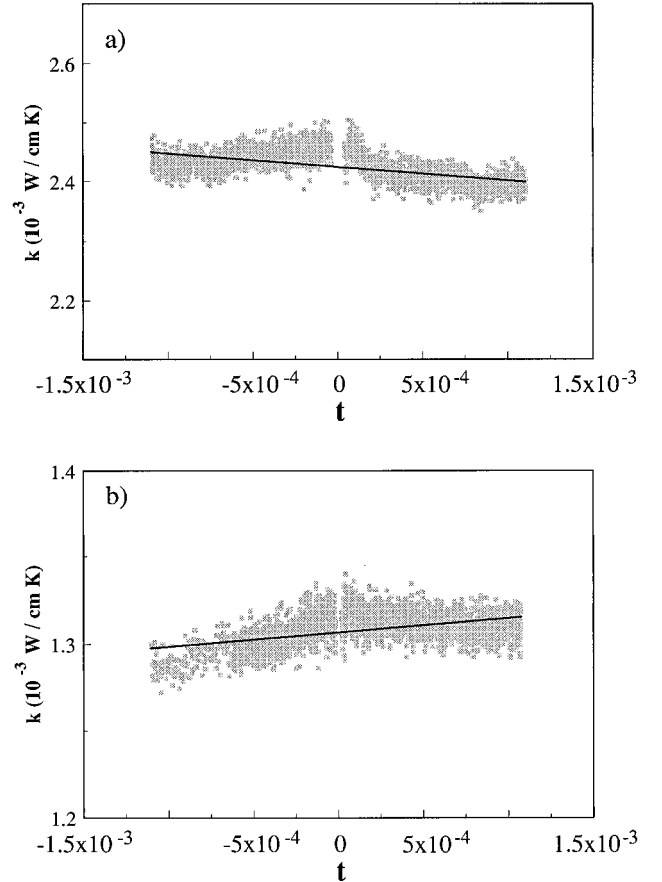


FIG. 5. 8CB thermal conductivity behavior vs reduced temperature  $t=(T-T_c)/T_c$  for homeotropic (a) and planar (b) aligned samples. Light grey squares represent the experimental data. Solid lines correspond to the best fits obtained from the expression  $k=H+G(T-T_c)$ , with parameter values given by fits 5A and 5B, respectively, of Table I.

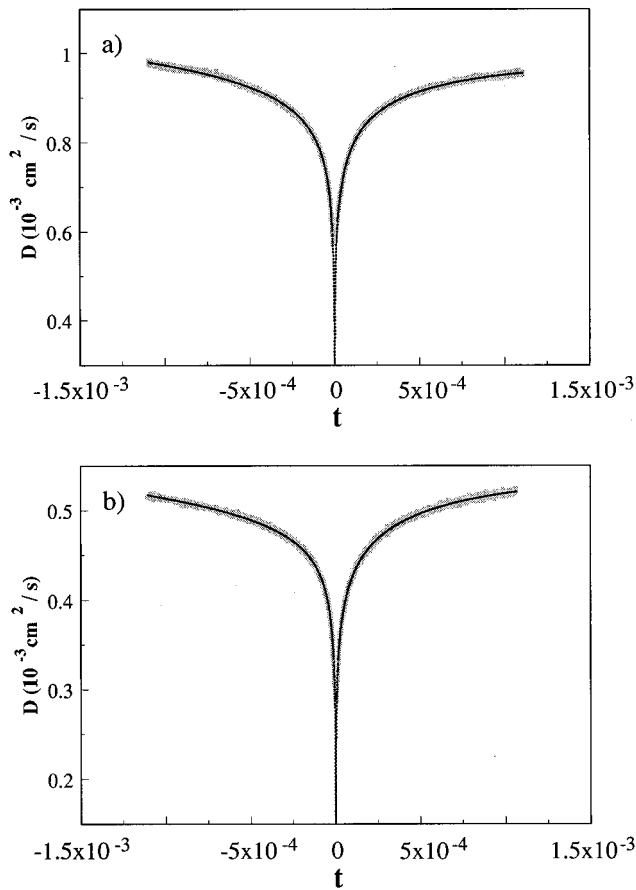


FIG. 6. 8CB thermal diffusivity behavior vs reduced temperature  $t=(T-T_C)/T_C$  for homeotropic (a) and planar (b) aligned samples. Light grey squares represent the experimental data. Solid lines correspond to the fits 3A and 3B of Table I. The dotted lines correspond to the reduced temperature regions which have not been considered in the fits.

noted that, at the AC transition, for example, a divergence which cannot be explained in terms of existing theories has been reported for some compounds [8]. It has also been shown [8] that this divergence becomes stronger when the mean-field tricritical point is approached, and the authors interpret this divergence in terms of an increasing importance of nondissipative couplings in the system.

Measurements in nonaligned 855 at the AN transition showed a flat thermal conductivity, while data in Fig. 5 show

a slight increase in  $k$  close to  $T_{AN}$ . The question now is whether this slight increase in  $k$  is an indication of additional nondissipative couplings coming into play when the tricritical point is approached or not. As already stated, it seems that something similar occurs at the AC transition where, close to the tricritical point, the divergence of  $k$  and  $D$  becomes stronger [8]. Measurements to check this issue further are presently underway, and will be presented in a forthcoming paper. It should finally be pointed out that previous measurements performed by the photoacoustic technique in non-aligned samples [14] led to a sharp and narrow peak in  $k$  at  $T_{AN}$ . It has been shown [12] that the photopyroelectric technique we have used in the present work is much more sensitive to the variation of thermal parameters than the gas-microphone one. A smaller temperature oscillation and therefore a smaller thermal gradient needs to be introduced in the sample during the measurement to have an adequate signal-to-noise ratio. It could therefore be that the peak shown in Ref. [14] is, at least partially, an artifact due to thermal gradients. In fact it appears in a reduced temperature region which was not considered when performing the fits on the  $c$  and  $D$  data because of the rounding effect.

## CONCLUSIONS

Simultaneous measurements of  $c$ ,  $k$ , and  $D$  in homeotropically and planar aligned 8CB samples have been reported. The same specific heat critical behavior has been obtained in two cases, and the results are in excellent agreement with the ones already reported in the literature [11]. The thermal diffusivity and the thermal conductivity have been measured in the temperature range 29–45 °C, where the sample undergoes the AN and NI phase transitions. The temperature dependence of the absolute values of the two quantities for the two aligned samples are similar to the ones already reported for *MBBA* and *OBBA* [7]. Moreover, it has been shown that  $D_{\parallel}$  and  $D_{\perp}$  have approximately the same critical behaviors around  $T_{AN}$ . This means that the anisotropy in the critical behaviors of  $\xi$  does not affect the transport thermal parameters critical behavior. This also means that all the couplings of long lived modes which are relevant in the heat transport process close to  $T_{AN}$  are isotropic. A rather smooth thermal conductivity has been found for both orientations over the transition temperature region, with only a minor increase close to  $T_{AN}$ . It is not clear at present if such an increase could be due to some as yet unknown physical reason, as in the case of the AC transition.

[1] C. W. Garland and G. Nounesis, *Phys. Rev. E* **49**, 2964 (1994).  
 [2] C. W. Garland, G. Nounesis, and K. J. Stine, *Phys. Rev. A* **39**, 4919 (1989).  
 [3] C. Bervillier, *Phys. Rev. B* **34**, 8141 (1986).  
 [4] R. Shasidhar, in *Phase Transition in Liquid Crystals*, edited by S. Martellucci and A. N. Chester (Plenum, New York, 1992), p. 227.  
 [5] T. C. Lubenski, *J. Chim. Phys.* **80**, 31 (1983).

[6] B. R. Patton and B. S. Andereck, *Phys. Rev. Lett.* **69**, 1556 (1992); B. S. Andereck and B. R. Patton, *Phys. Rev. E* **49**, 1393 (1994).  
 [7] F. Rondelez, W. Urbach, and H. Hervet, *Phys. Rev. Lett.* **41**, 1058 (1978); W. Urbach, H. Hervet, and F. Rondelez, *Mol. Cryst. Liq. Cryst.* **46**, 209 (1978).  
 [8] E. K. Hobbie, H. Y. Liu, C. C. Huang, Ch. Bahr, and G. Heppke, *Phys. Rev. Lett.* **67**, 1771 (1991).

- [9] M. Marinelli, F. Mercuri, U. Zammit, and F. Scudieri, Phys. Rev. E **53**, 701 (1996).
- [10] P. C. Hohenberg and B. I. Halperin, Rev. Mod. Phys. **49**, 435 (1977).
- [11] J. Thoen, H. Marynissen, and W. Van Dael, Phys. Rev. A **26**, 2886 (1982); Phys. Rev. Lett. **52**, 204 (1984).
- [12] M. Marinelli, U. Zammit, F. Mercuri, and R. Pizzoferrato, J. Appl. Phys. **72**, 1096 (1992).
- [13] A. Mandelis and M. M. Zver, J. Appl. Phys. **57**, 4421 (1985).
- [14] U. Zammit, M. Marinelli, R. Pizzoferrato, F. Scudieri, and S. Martellucci, Phys. Rev. A **41**, 1153 (1990).